J. Fluid Mech. (2016), *vol.* 802, R2, doi:10.1017/jfm.2016.472

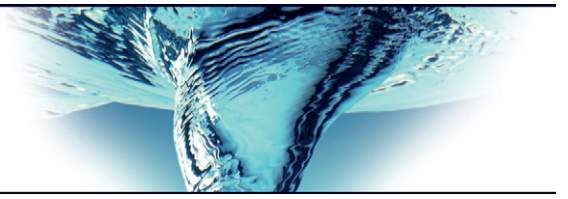

Revisiting the subgrid-scale Prandtl number for large-eddy simulation

Dan Li†

Department of Earth and Environment, Boston University, Boston, MA 02215, USA

(Received 2 June 2016; revised 8 July 2016; accepted 10 July 2016)

The subgrid-scale (SGS) Prandtl number (Pr) is an important parameter in large-eddy simulation. Prior models often assume that the '$-5/3$' inertial subrange scaling applies to the wavenumber range from 0 to k_Δ (the wavenumber corresponding to the filter scale Δ) and yield a Pr that is stability-independent and scale-invariant, which is inconsistent with experimental data and the results of dynamic models. In this study, the SGS Prandtl number is revisited by solving the co-spectral budgets of momentum and heat fluxes in an idealized but thermally stratified atmospheric surface layer. The SGS Prandtl number from the co-spectral budget model shows a strong dependence on the atmospheric stability and increases (decreases) as the atmosphere becomes stable (unstable), which is in good agreement with recent field experimental data. The dependence of Pr on the filter scale is also captured by the co-spectral budget model: as the filter scale becomes smaller, the SGS Prandtl number decreases. Finally, the value of SGS Prandtl number under neutral conditions is shown to be caused by the dissimilarity between momentum and heat in the pressure decorrelation term and the flux transfer term. When the dissimilarity exists only in the flux transfer term, the fact that under neutral conditions the SGS Prandtl number is usually smaller than the turbulent Prandtl number for Reynolds-averaged Navier–Stokes simulations is an indication of a stronger spectral transfer coefficient for heat than for momentum. The model proposed in this study can be readily implemented.

Key words: atmospheric flows, stratified turbulence, turbulence modelling

1. Introduction

Large-eddy simulation (LES) has become a widely used numerical technique for studying turbulent flows. Turbulence often consists of a wide range of scales, which increases with the Reynolds number (Tennekes & Lumley 1972). For example, the largest scale in the atmospheric boundary layer is of the order of 1 km, while the

† Email address for correspondence: lidan@bu.edu

smallest scale is of the order of 1 mm (Stull 1988). The essence of LES is to resolve the large scales but parameterize the effects of small scales using so-called subgrid-scale (SGS) models (Pope 2000). This is motivated by the turbulent energy cascade in which the large scales extract energy from the mean flow and transfer it to the small scales. As a result, the small scales are less affected by the boundary conditions and should thus be easier to model.

In particular, the pioneering work of Kolmogorov (1941) hypothesized that, if a sufficiently large scale separation exists between the largest scale and the smallest scale (i.e. the turbulent flow has a sufficiently large Reynolds number like the flow in the atmospheric boundary layer), then an inertial subrange exists in which turbulence is homogeneous and isotropic. His work further demonstrated that the turbulent kinetic energy (TKE) spectra in the inertial subrange follow the nowadays well-known '$-5/3$' scaling. The temperature spectra in the inertial subrange were later found to also follow such scaling by Obukhov (1949) and Corrsin (1951). The Kolmogorov–Obukhov–Corrsin theory provides the basis for developing SGS models.

The most widely used SGS model is arguably the Smagorinsky model (Smagorinsky 1963), which is analogous to the mixing-length model proposed by Prandtl for Reynolds-averaged Naiver–Stokes (RANS) simulations. In this model, the SGS momentum (heat) flux is assumed to be proportional to the resolved velocity (temperature) gradient and the proportionality is termed SGS eddy viscosity (eddy diffusivity). The ratio of SGS eddy viscosity and eddy diffusivity is called the SGS Prandtl number, which is the focus of this study. Lilly was the first to estimate the SGS eddy viscosity based on the Kolmogorov theory (Lilly 1967), and others extended the analysis to the SGS eddy diffusivity (Schumann, Grötzbach & Kleiser 1980; Moeng & Wyngaard 1988; Mason 1989). However, such analysis yielded an SGS Prandtl number that is both stability- (or buoyancy-) independent and scale-invariant, which is inconsistent with recent field experiments (Porté-Agel *et al.* 2001; Bou-Zeid *et al.* 2008; Vercauteren *et al.* 2008; Bou-Zeid *et al.* 2010) and new computational developments (Porté-Agel 2004; Basu & Porté-Agel 2006; Stoll & Porté-Agel 2006, 2008; Calaf, Parlange & Meneveau 2011) showing that the SGS Prandtl number is stability-dependent and varies with scales.

In this study, the SGS Prandtl number is revisited by solving the SGS co-spectral budgets of momentum and heat fluxes. It is shown that even under stationary and horizontally homogeneous conditions that are often assumed to be associated with high-Reynolds-number flows in the atmospheric surface layer (ASL, which is the lowest 10 %–20 % of the atmospheric boundary layer and corresponds to the logarithmic region in wall-bounded turbulence), the SGS Prandtl number is strongly impacted by thermal stratification and the filter scale. This co-spectral budget model is in good agreement with recent field experimental data collected in the ASL and can be readily implemented in LES.

2. Theory

The SGS turbulent momentum (τ) and heat (h) fluxes are modelled as

$$\tau_{ij} = -2c_s^2\Delta^2|\widetilde{S}|\widetilde{S}_{ij}, \tag{2.1}$$

$$h_i = -Pr^{-1}c_s^2\Delta^2|\widetilde{S}|\widetilde{D}_i, \tag{2.2}$$

respectively, where $|\widetilde{S}| = (2\widetilde{S}_{ij}\widetilde{S}_{ij})^{1/2}$, $\widetilde{S}_{ij} = 0.5(\partial\widetilde{u}_i/\partial x_j + \partial\widetilde{u}_j/\partial x_i)$, $\widetilde{D}_i = \partial\widetilde{\theta}/\partial x_i$, u_i is the velocity, θ is the potential temperature, c_s is the Smagorinsky coefficient, Δ is the filter scale and Pr is the SGS Prandtl number. The tilde ($\sim$) denotes the filtering operation.

2.1. *Prior model*

Theoretical derivations of the SGS Prandtl number can be found in previous studies (Schumann *et al.* 1980; Moeng & Wyngaard 1988; Mason 1989), all of which were built on Lilly's thinking (Lilly 1967). By assuming that the inertial subrange spectra of TKE ($E_{TKE} = C_{TKE}\epsilon^{2/3}k^{-5/3}$) and temperature ($E_{TT} = C_T\epsilon^{-1/3}\epsilon_T k^{-5/3}$) apply to the wavenumber range from 0 to k_Δ ($=\pi/\Delta$), one arrives at

$$\tilde{S}^2 = 2\int_0^{k_\Delta} k^2 E_{TKE}(k)\,\mathrm{d}k = \frac{3}{2}C_{TKE}\epsilon^{2/3}k_\Delta^{4/3}, \tag{2.3}$$

$$\tilde{D}^2 = 2\int_0^{k_\Delta} k^2 E_{TT}(k)\,\mathrm{d}k = \frac{3}{2}C_T\epsilon^{-1/3}\epsilon_T k_\Delta^{4/3}, \tag{2.4}$$

where $|\widetilde{D}| = (\widetilde{D}_i\widetilde{D}_i)^{1/2}$, k is the wavenumber, C_{TKE} is the Kolmogorov constant for TKE, C_T is the Obukhov–Corrsin constant, and ϵ and ϵ_T are dissipation rates for TKE and temperature variance, respectively. It is pointed out here that the original work of Kolmogorov assumed that ϵ is the dissipation rate of the ensemble mean TKE, but here ϵ (and ϵ_T) is the dissipation rate for the SGS TKE (and temperature variance). Assuming that the budgets for SGS TKE and temperature variance are in equilibrium and neglecting the effect of thermal stratification, one can show that $\epsilon/\epsilon_T = Pr\tilde{S}^2/\tilde{D}^2$ (Schumann *et al.* 1980; Moeng & Wyngaard 1988; Mason 1989). As such,

$$Pr = \frac{C_T}{C_{TKE}} \approx 0.47. \tag{2.5}$$

The assumption that the inertial subrange spectra apply to the wavenumber range from 0 to k_Δ is clearly questionable. The above model also results in a Pr that is independent of stability and k_Δ, which is inconsistent with recent field experiments (Porté-Agel *et al.* 2001; Bou-Zeid *et al.* 2008; Vercauteren *et al.* 2008; Bou-Zeid *et al.* 2010) and dynamic model results (Porté-Agel 2004; Basu & Porté-Agel 2006; Stoll & Porté-Agel 2006, 2008; Calaf *et al.* 2011) showing that Pr is stability-dependent and varies with scales.

Deardorff (1973, 1980) tried to account for the impact of stable stratification on Pr based on heuristic arguments and used a Pr that gradually increased from 1/3 under unstable and neutral conditions to 1 under very stable conditions. Others used empirical functions to account for the effect of stability on Pr (Brown, Derbyshire & Mason 1994; Mason & Brown 1999). Schumann (1991) solved the SGS momentum and heat flux budgets algebraically in the physical space, which yielded a Pr that increases with stable stratification. This study builds on the study by Schumann (1991) but solves the momentum and heat flux budgets in the spectral space under both stable and unstable stratification and considers the influence of the filter scale on Pr.

2.2. *The co-spectral budget model*

To simplify the problem, let's consider the SGS momentum and heat fluxes in a high-Reynolds-number ASL flow that is stationary, horizontally homogeneous and without subsidence, which can be linked to their co-spectra (F_{uw} and F_{wT}) via $\tau_{13} = \int_{k_\Delta}^{\infty} F_{uw}(k)\,\mathrm{d}k$ and $h_3 = \int_{k_\Delta}^{\infty} F_{wT}(k)\,\mathrm{d}k$, respectively. Here k is interpreted as a one-dimensional wavenumber in the longitudinal direction since most field experiments calculate spectra and co-spectra from single-point measurements of time

series using Taylor's hypothesis of frozen turbulence (Taylor 1938) to convert time to one-dimensional longitudinal wavenumber. The co-spectral budgets of momentum and heat fluxes under the same assumptions are as follows (Panchev 1971; Bos *et al.* 2004; Katul *et al.* 2013, 2014):

$$\frac{\partial F_{uw}(k)}{\partial t} = 0 = P_{uw}(k) + T_{uw}(k) + \pi_u(k) + \beta F_{uT}(k) - 2\nu k^2 F_{uw}(k), \tag{2.6}$$

$$\frac{\partial F_{wT}(k)}{\partial t} = 0 = P_{wT}(k) + T_{wT}(k) + \pi_T(k) + \beta E_{TT}(k) - (\nu + D_m)k^2 F_{wT}(k). \tag{2.7}$$

The terms on the left-hand side of the equations represent temporal changes in the co-spectra. The terms on the right-hand side represent (in order): shear production (P), flux transfer (T), pressure decorrelation (π), buoyancy (βF_{uT} and βE_{TT}) and molecular destruction. The exact formulation for each term can be found elsewhere (Katul *et al.* 2013, 2014). $\beta = g/\tilde{\theta}$ is the buoyancy parameter and g is the gravitational acceleration. The effect of co-spectra between the longitudinal velocity and temperature (F_{uT}) is assumed to be sufficiently small compared to P_{uw} as demonstrated by direct numerical simulations and scaling arguments (Katul *et al.* 2014). ν is the kinematic viscosity and D_m is the molecular thermal diffusivity. The molecular destruction terms are also assumed to be small since they are significant only at scales comparable to η, the Kolmogorov length scale that is of the order of 1 mm in the ASL. This requires that $\Delta \gg \eta$, which is not always the case in LES. With these additional assumptions, the co-spectral budgets of momentum and heat fluxes are simplified to

$$P_{uw}(k) + T_{uw}(k) + \pi_u(k) = 0, \tag{2.8}$$

$$P_{wT}(k) + T_{wT}(k) + \pi_T(k) + \beta E_{TT}(k) = 0. \tag{2.9}$$

By performing direct Fourier transformation of the shear production terms in the physical space and invoking the Rotta model (Pope 2000) for parameterizing the pressure decorrelation terms (π_u and π_T) and a spectral gradient diffusion model (Bos *et al.* 2004) for parameterizing the flux transfer terms (T_{uw} and T_{wT}),

$$P_{uw}(k) = -E_{ww}(k)S, \tag{2.10}$$

$$P_{wT}(k) = -E_{ww}(k)\Gamma, \tag{2.11}$$

$$\pi_u(k) = -A_U \frac{F_{uw}(k)}{\epsilon^{-1/3}k^{-2/3}} - C_{IU}P_{uw}(k), \tag{2.12}$$

$$\pi_T(k) = -A_T \frac{F_{wT}(k)}{\epsilon^{-1/3}k^{-2/3}} - C_{IT}P_{wT}(k), \tag{2.13}$$

$$T_{uw}(k) = -A_{UU}\frac{\partial}{\partial k}(\varepsilon^{1/3}\ k^{5/3}F_{uw}(k)), \tag{2.14}$$

$$T_{wT}(k) = -A_{TT}\frac{\partial}{\partial k}(\varepsilon^{1/3}\ k^{5/3}F_{wT}(k)), \tag{2.15}$$

equations (2.8) and (2.9) reduce to

$$\frac{\partial F_{uw}(k)}{\partial k} + D_1 k^{-1} F_{uw}(k) = D_2 E_{ww}(k)k^{-5/3}, \tag{2.16}$$

$$\frac{\partial F_{wT}(k)}{\partial k} + D_3 k^{-1} F_{wT}(k) = D_4 E_{ww}(k)k^{-5/3} + D_5 E_{TT}(k)k^{-5/3}, \tag{2.17}$$

where

$$\left.\begin{aligned} D_1 = \frac{A_U}{A_{UU}} + \frac{5}{3}, \quad D_2 = -\frac{(1-C_{IU})S}{A_{UU}\epsilon^{1/3}}, \quad D_3 = \frac{A_T}{A_{TT}} + \frac{5}{3}, \\ D_4 = -\frac{(1-C_{IT})\Gamma}{A_{TT}\epsilon^{1/3}}, \quad D_5 = \frac{\beta}{A_{TT}\epsilon^{1/3}}, \end{aligned}\right\} \tag{2.18}$$

E_{ww} is the spectrum of vertical velocity, E_{TT} is the spectrum of temperature, $S = \mathrm{d}\tilde{u}/\mathrm{d}z$ and $\Gamma = \mathrm{d}\tilde{\theta}/\mathrm{d}z$ are the resolved longitudinal velocity and temperature gradients in the vertical (z) direction, respectively, A_U and A_T are the Rotta constants (Pope 2000), C_{IU} and C_{IT} are constants associated with isotropization of production terms (Pope 2000) whose value can be determined using Rapid Distortion Theory for homogeneous turbulence (=0.6), and A_{UU} and A_{TT} are constants in the gradient diffusion model. These constants are not necessarily identical for momentum and heat (Li, Katul & Bou-Zeid 2015*a*). Similarity between momentum and heat (i.e. Reynolds analogy) will be assumed for Rotta and isotropization constants only when analysing the influence of A_{TT}/A_{UU} on Pr, as shall be seen later.

The above equations for $F_{uw}(k)$ and $F_{wT}(k)$ can be solved once $E_{ww}(k)$ and $E_{TT}(k)$ are known. It is convenient to begin with a general power-law formulation with $E_{ww}(k) = C_{ww}k^{-\alpha}$ and $E_{TT}(k) = C_{TT}k^{-\gamma}$, where α and γ are spectral scaling exponents and C_{ww} and C_{TT} are normalization factors, which yield

$$F_{uw}(k) = \frac{D_2}{-\alpha - 2/3 + D_1} C_{ww}k^{-\alpha-2/3} + E_1 k^{-D_1}, \tag{2.19}$$

$$F_{wT}(k) = \frac{D_4}{-\alpha - 2/3 + D_3} C_{ww}k^{-\alpha-2/3} + \frac{D_5}{-\gamma - 2/3 + D_3} C_{TT}k^{-\gamma-2/3} + E_2 k^{-D_3}, \tag{2.20}$$

where E_1 and E_2 are integration constants appearing due to the consideration of flux transfer among scales. To prohibit up-gradient fluxes generated by shear production and buoyancy terms, $D_1 > \alpha + 2/3$ and $D_3 > \max(\alpha + 2/3, \gamma + 2/3)$. That is, $A_U/A_{UU} > \alpha - 1$ and $A_T/A_{TT} > \max(\alpha - 1, \gamma - 1)$.

In the inertial subrange, $\alpha = \gamma = 5/3$, $C_{ww} = C_o\epsilon^{2/3}$ (where C_o is the Kolmogorov constant for the vertical velocity variance) and $C_{TT} = C_T\epsilon_T\epsilon^{-1/3}$. Hence $A_U/A_{UU} > 2/3$ and $A_T/A_{TT} > 2/3$. Further assuming that the inertial subrange scaling applies for $k > k_\Delta$, which requires the Ozmidov scale to be larger than Δ (Bou-Zeid *et al.* 2010; Katul *et al.* 2014; Li, Salesky & Banerjee 2016), the SGS momentum and heat fluxes can be evaluated:

$$\tau_{13} = \int_{k_\Delta}^{\infty} F_{uw}(k)\,\mathrm{d}k = \frac{D_2}{(D_1 - 7/3)(4/3)} C_o\epsilon^{2/3}{k_\Delta}^{-4/3} + \frac{E_1}{D_1 - 1}{k_\Delta}^{-D_1+1}, \tag{2.21}$$

$$h_3 = \int_{k_\Delta}^{\infty} F_{wT}(k)\,\mathrm{d}k = \frac{D_4}{(D_3 - 7/3)(4/3)} C_o\epsilon^{2/3}{k_\Delta}^{-4/3}Q + \frac{E_2}{D_3 - 1}{k_\Delta}^{-D_3+1}, \tag{2.22}$$

where

$$Q = 1 - \frac{1}{1 - C_{IT}}\frac{C_T}{C_o}\frac{R_f}{(1 - R_f)}. \tag{2.23}$$

Note the above integration implicitly assumes that S and Γ are independent of k and hence they can be viewed as the longitudinal velocity and temperature gradients 'imposed' by the resolved flow on the SGS component. R_f is the flux Richardson number ($=\beta h_3/(S\tau_{13})$), which indicates the thermal stratification ($R_f > 0$ denotes stable

stratification and $R_f < 0$ denotes unstable stratification). A critical assumption needed in the derivation of Q is that the budgets for SGS TKE and temperature variance are in equilibrium (Katul *et al.* 2014).

In the following, two cases are considered. The first assumes $E_1 = E_2 = 0$, which yields that F_{uw} and F_{wT} follow the '$-7/3$' scaling in the inertial subrange. This is supported by many theoretical and experimental studies, especially for F_{uw} (Lumley 1964; Kaimal & Finnigan 1994; Saddoughi & Veeravalli 1994). The second assumes that $E_1 = 0$ but $E_2 \neq 0$, that is, F_{uw} follow the '$-7/3$' scaling but F_{wT} are 'contaminated' by some anomalous scaling (Bos *et al.* 2004; Bos, Touil & Bertoglio 2005; Bos & Bertoglio 2007). Note E_1 is always 0 because the effects of E_1 and E_2 are taken into account, as shall be seen later, by assuming that they are proportional to the buoyancy term, which has already been neglected in the budget of F_{uw}.

2.3. *Case 1:* $E_1 = E_2 = 0$

With $E_1 = E_2 = 0$, the co-spectral budget model immediately gives

$$Pr = \frac{-\tau_{13}/S}{-h_3/\Gamma} = Pr_{neu} Q^{-1} = Pr_{neu} \left(1 - \frac{1}{1 - C_{IT}} \frac{C_T}{C_o} \frac{R_f}{(1 - R_f)}\right)^{-1}, \tag{2.24}$$

where Pr_{neu} is the SGS Prandtl number under neutral conditions ($R_f = 0$) given by

$$Pr_{neu} = \frac{A_{TT}(1 - C_{IU})}{A_{UU}(1 - C_{IT})} \frac{(A_T/A_{TT} - 2/3)}{(A_U/A_{UU} - 2/3)}. \tag{2.25}$$

From (2.24) one can see that the SGS Prandtl number is dependent on the atmospheric stability (represented by R_f) through Q, which is fully described by three phenomenological constants (i.e. the Kolmogorov constant C_o, the Obukhov–Corrsin constant C_T and the isotropization constant in the Rotta model C_{IT}). In this study, $C_o = 0.65$, $C_T = 0.8$ and $C_{IT} = 0.6$ are used (Sreenivasan 1995, 1996; Pope 2000). This is similar to previous results for the turbulent Prandtl number in RANS modelling (Katul *et al.* 2014; Li, Katul & Zilitinkevich 2015*b*). It is interesting to see that Q depends on the Kolmogorov constant for the vertical velocity variance ($C_o = (24/55)C_{TKE}$) instead of that for TKE (C_{TKE}). This is due to the fact that the shear production terms in the co-spectral budgets (P_{uw} and P_{wT}) involve only the vertical velocity spectra. Note that the SGS Prandtl number from (2.24) remains scale-invariant.

2.4. *Case 2:* $E_1 = 0$ *and* $E_2 \neq 0$

If $E_1 = 0$ but $E_2 \neq 0$, one then obtains $Pr = Pr_{neu}(Q + A_s)^{-1}$, where

$$A_s = \frac{4}{3} \frac{(A_T/A_{TT} - 2/3)}{(A_T/A_{TT} + 2/3)} k_\Delta{}^{-(A_T/A_{TT}) + (2/3)} \frac{E_2/\Gamma}{D_4 C_{ww}/\Gamma}. \tag{2.26}$$

For convenience, let's write $E_2 = A_{E_2} D_5 C_{TT}$, that is, the impact of E_2 on F_{wT} is proportional to the buoyancy term as alluded to earlier. It is assumed to have the opposite sign to the production term (i.e. $A_{E_2} > 0$ for $R_f > 0$ and $A_{E_2} < 0$ for $R_f < 0$) since the flux transfer term, which gives rise to E_2, effectively reduces the variability of flux across scales. Substituting the expression for E_2 results in

$$Pr = Pr_{neu} \left(1 - (1 + B_{E_2}) \frac{1}{1 - C_{IT}} \frac{C_T}{C_o} \frac{R_f}{(1 - R_f)}\right)^{-1}, \tag{2.27}$$

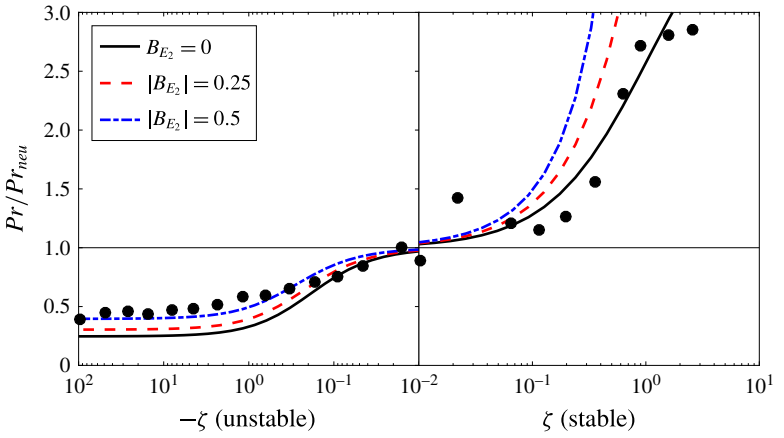

FIGURE 1. Comparison between modelled (lines) and measured (circles) Pr/Pr_{neu} as a function of the stability parameter ζ. Observational data are taken from field experiments over a lake (Bou-Zeid *et al.* 2008) and a glacier (Bou-Zeid *et al.* 2010).

where

$$B_{E_2} = \frac{4}{3}\frac{(A_T/A_{TT} - 2/3)}{(A_T/A_{TT} + 2/3)} A_{E_2} k_\Delta{}^{-(A_T/A_{TT})+(2/3)}. \tag{2.28}$$

It is clear that the SGS Prandtl number is now also dependent on the filter scale Δ through B_{E2}. When $B_{E_2} = 0$, equation (2.27) recovers (2.24). Since $A_{E2}R_f > 0$ and thus $B_{E2}R_f > 0$, it is straightforward to show that, at a given R_f, Pr decreases as k_Δ increases (or as Δ decreases).

3. Results

First, the stability dependence of Pr is examined without considering the influence of the filter scale. As such, equation (2.27) with prescribed values of B_{E_2} is used. Figure 1 shows the comparison between modelled (lines) and measured (circles) Pr/Pr_{neu} as a function of the stability parameter ζ in Monin–Obukhov similarity theory (Monin & Obukhov 1954). ζ is used here instead of R_f because it is often reported in ASL field experiments. R_f can be related to ζ through $R_f = \zeta/\phi_m$, where $\phi_m = \kappa z S/(-\tau_{13})^{1/2}$ is the normalized longitudinal velocity gradient for which the Businger–Dyer relation is used (Businger *et al.* 1971; Högström 1988), κ is the von Kármán constant and z is the height from the ground. It is clear that the model captures the general trend of SGS Prandtl number reported in recent field experiments (Bou-Zeid *et al.* 2008, 2010). Each circle here is the median value of measured Pr over a small range of ζ. The model with $B_{E_2} = 0$ better captures the trend under stable conditions while $|B_{E_2}| = 0.5$ (i.e. $B_{E_2} = -0.5$ when $\zeta < 0$) better captures the trend under unstable conditions, suggesting that the flux transfer term, which gives rise to B_{E_2}, is more significant under unstable conditions. This is consistent with many previous studies underscoring the increasingly important role of the flux transport term in the physical domain as the atmosphere becomes more unstable (Stull 1988).

Second, the sensitivity of Pr to the filter scale (Δ) is investigated. Unlike figure 1 where only one input parameter (B_{E2}) was required, the model now needs two input parameters (A_{E_2} and A_T/A_{TT}). These two need to satisfy $A_{E_2}\zeta > 0$ and $A_T/A_{TT} > 2/3$. It can be shown that the co-spectral budget model always yields a decreasing Pr as

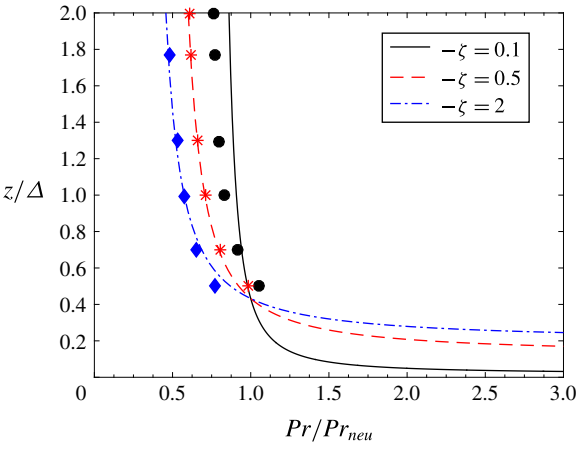

FIGURE 2. Comparison between modelled (lines) and measured (symbols) Pr/Pr_{neu} as a function of z/Δ for three stability regimes. $A_{E_2} = -2.7$ and $A_T/A_{TT} = 1.08$ are used in the model. Observational data are taken from field experiments over a lake (Vercauteren *et al.* 2008).

the filter scale becomes smaller under both stable and unstable conditions. Figure 2 shows three examples under unstable conditions with field experimental data from Vercauteren *et al.* (2008). One can see that both the model and data indicate that the SGS Prandtl number decreases as the filter scale decreases (i.e. as z/Δ increases), which is also consistent with other experimental studies (Porté-Agel *et al.* 2001) and the results of dynamic models (Basu & Porté-Agel 2006). Note that the observational data were averaged over three stability regimes ($0 < -\zeta < 0.1$, $0.1 < -\zeta < 1$, $1 < -\zeta$) and thus three predictions with different stability parameters are shown in figure 2. It should be also pointed out that Δ used in the analysis of observational data might not always be in the inertial subrange. Here $A_{E_2} = -2.7$ and $A_T/A_{TT} = 1.08$ are used in the model but it is not the purpose of this study to calibrate these two parameters using experimental data. Rather the goal here is to study the behaviour of the co-spectral budget model.

The above results focus on the SGS Prandtl number normalized by its neutral value. Here the neutral value of SGS Prandtl number (Pr_{neu}) is examined. As already mentioned, earlier theoretical work obtained a value of about 0.47 as the ratio of the Obukhov–Corrsin constant and the Kolmogorov constant for TKE (Schumann *et al.* 1980; Moeng & Wyngaard 1988; Mason 1989). However, there is no consensus on the exact value of Pr_{neu}. For example, 1/3 was used by Deardorff (1973, 1980). In addition, the variability of Pr_{neu} remains very large in experimental data (Pitsch & Steiner 2000; Porté-Agel *et al.* 2001; Bou-Zeid *et al.* 2008, 2010; Vercauteren *et al.* 2008). It can be seen from equation (2.25) that Pr_{neu} from the co-spectral budget model is dependent on the dissimilarity between momentum and heat in the pressure decorrelation and flux transfer terms. Figure 3 shows the SGS Pr_{neu} normalized by its counterpart for RANS modelling when $A_U/A_T = 1$ and $(1 - C_{IU})/(1 - C_{IT}) = 1$ (that is, assuming similarity between momentum and heat in the Rotta model for pressure decorrelation terms). Note that the turbulent Prandtl number for RANS modelling has been previously studied using a similar co-spectral budget model (Katul *et al.* 2014; Li *et al.* 2015*a*,*b*). It is clear that the value of A_{TT}/A_{UU}, which indicates the momentum–heat dissimilarity in the flux transfer term, has a significant impact on the

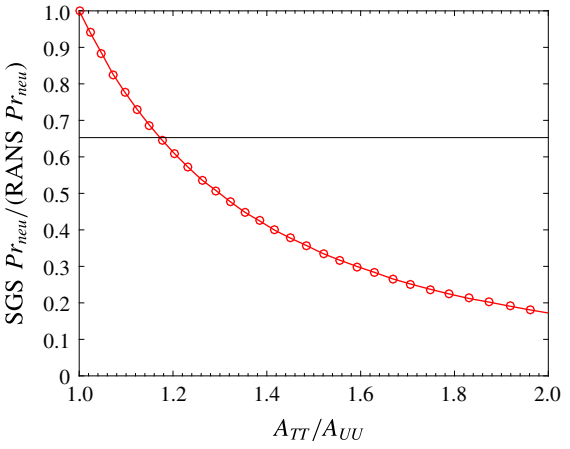

FIGURE 3. The neutral value of SGS Prandtl number normalized by the neutral value of Reynolds-averaged turbulent Prandtl number as a function of A_{TT}/A_{UU}. The black line denotes a ratio of 0.47/0.72.

SGS Pr_{neu}. The SGS Pr_{neu} is only equal to its counterpart in RANS when $A_{TT}/A_{UU} = 1$, and the ratio of the two decreases as A_{TT}/A_{UU} increases. Typical values used in the literature (i.e. $Pr_{neu} = 0.47$ and 0.72 for SGS and RANS modelling, respectively) indicate that $A_{TT}/A_{UU} \approx 1.18$, that is, a stronger spectral transfer coefficient for heat than momentum.

4. Conclusions and discussion

The subgrid-scale Prandtl number (Pr), which is an important parameter in LES, is revisited by solving the co-spectral budgets of momentum and heat fluxes. The co-spectral budget model assumes that the inertial subrange '$-5/3$' scaling applies for $k > k_\Delta$ (the wavenumber corresponding to the filter scale Δ), as compared to prior models that assume that the '$-5/3$' scaling applies for $0 < k < k_\Delta$. The model also invokes the Rotta model for parameterizing the pressure decorrelation term and a gradient diffusion model for parameterizing the flux transfer term. The resulting Pr is stability- and scale-dependent, which is contrary to prior Pr estimates that are stability-independent and scale-invariant. More specifically, Pr increases (decreases) as the atmosphere becomes stable (unstable) and decreases as the filter scale becomes smaller, which is in good agreement with field experimental data and the results of dynamic models.

The influence of stability on Pr comes from the dependence of Pr on the resolved longitudinal velocity and temperature gradients, which are strongly affected by thermal stratification. In this study, the resolved longitudinal velocity and temperature gradients are 'imposed' on the SGS flow. This assumption is often made for SGS (and RANS) modelling to simplify the analysis but may not always be realistic, especially for more complex turbulent flows. The trend of Pr with stability suggests that buoyancy production (destruction) of TKE enhances (reduces) the turbulent transport efficiency of heat compared to momentum (Li & Bou-Zeid 2011; Li, Katul & Bou-Zeid 2012) even at subgrid scales.

On the other hand, the dependence of Pr on the filter scale, even when the filter scale is within the inertial subrange, stems from the fact that the co-spectra

of momentum and heat fluxes have different scaling laws, which is further caused by the dissimilarity between the scale-wise transfer of momentum and heat and their interactions with pressure fluctuations. Unlike the energy spectra, which have a well-established '$-5/3$' scaling in the inertial subrange, the flux co-spectra seem to show non-universal behaviours (Bos *et al.* 2004, 2005; Bos & Bertoglio 2007). The neutral value of Pr is also dependent on the momentum–heat dissimilarity in the Rotta model and the gradient diffusion model. If Reynolds analogy is assumed in the Rotta model, the fact that under neutral conditions the SGS Prandtl number is smaller than the Reynolds-averaged turbulent Prandtl number is an indication of a stronger spectral transfer coefficient for heat than for momentum.

The model (2.27) proposed here can be readily implemented and is mainly dependent on three well-established phenomenological constants (i.e. the Kolmogorov constant for the vertical velocity variance, the Obukhov–Corrsin constant and the isotropization constant in the Rotta model). Even for dynamic models, this parameterization for Pr can avoid a dynamic determination of SGS heat diffusivity. To account for the stability effect, $B_{E_2} = 0$ and $B_{E_2} = -0.5$ are recommended for stable and unstable conditions, respectively. The model can also account for the scale dependence given the values of A_{E_2} and A_T/A_{TT}, which need further investigations. The exact value of Pr under neutral conditions also remains an open question.

Although the model is developed and validated in the atmospheric surface layer, it may be applied to more general conditions (at least as a first-order correction to prior models) if the Reynolds number is sufficiently large and the filter scale is within the inertial subrange (but not too close to the Kolmogorov scale) so that most assumptions made here remain valid. A useful extension of this work would be to compare the performance of the co-spectral budget model to prior models and empirical parameterizations (Brown *et al.* 1994; Mason & Brown 1999) for simulation of stratified turbulent flows.

Acknowledgements

The author thanks Professor E. Bou-Zeid from Princeton University for providing the observational data used in figure 1 and for inspiring discussions. Comments and suggestions from the two reviewers are greatly appreciated.

References

Basu, S. & Porté-Agel, F. 2006 Large-eddy simulation of stably stratified atmospheric boundary layer turbulence: a scale-dependent dynamic modeling approach. *J. Atmos. Sci.* **63**, 2074–2091.

Bos, W. J. T. & Bertoglio, J. P. 2007 Inertial range scaling of scalar flux spectra in uniformly sheared turbulence. *Phys. Fluids* **19**, 025104.

Bos, W. J. T., Touil, H. & Bertoglio, J. P. 2005 Reynolds number dependency of the scalar flux spectrum in isotropic turbulence with a uniform scalar gradient. *Phys. Fluids* **17** (12), 125108.

Bos, W. J. T., Touil, H., Shao, L. & Bertogli, J. P. 2004 On the behavior of the velocity–scalar cross correlation spectrum in the inertial range. *Phys. Fluids* **16**, 3818–3823.

Bou-Zeid, E., Higgins, C., Huwald, H., Parlange, M. B. & Meneveau, C. 2010 Field study of the dynamics and modelling of subgrid scale turbulence in a stable atmospheric surface layer over a glacier. *J. Fluid Mech.* **665**, 480–515.

Bou-Zeid, E., Vercauteren, N., Parlange, M. B. & Meneveau, C. 2008 Scale dependence of subgrid-scale model coefficients: an *a priori* study. *Phys. Fluids* **20** (11), 115106.

Brown, A. R., Derbyshire, S. H. & Mason, P. J. 1994 Large-eddy simulation of stable atmospheric boundary layers with a revised stochastic subgrid model. *Q. J. R. Meterol. Soc.* **120** (520), 1485–1512.

BUSINGER, J. A., WYNGAARD, J. C., IZUMI, Y. & BRADLEY, E. F. 1971 Flux-profile relationships in the atmospheric surface layer. *J. Atmos. Sci.* **28** (2), 181–191.

CALAF, M., PARLANGE, M. B. & MENEVEAU, C. 2011 Large eddy simulation study of scalar transport in fully developed wind-turbine array boundary layers. *Phys. Fluids* **23** (12), 126603.

CORRSIN, S. 1951 On the spectrum of isotropic temperature fluctuations in an isotropic turbulence. *J. Appl. Phys.* **22** (4), 469–473.

DEARDORFF, J. W. 1973 The use of subgrid transport equations in a three-dimensional model of atmospheric turbulence. *Trans. ASME J. Fluids Engng* **95** (3), 429–438.

DEARDORFF, J. W. 1980 Stratocumulus-capped mixed layers derived from a three-dimensional model. *Boundary-Layer Meteorol.* **18** (4), 495–527.

HÖGSTRÖM, U. L. F. 1988 Non-dimensional wind and temperature profiles in the atmospheric surface layer: a re-evaluation. In *Topics in Micrometeorology. A Festschrift for Arch Dyer*, pp. 55–78. Springer.

KAIMAL, J. C. & FINNIGAN, J. C. 1994 *Atmospheric Boundary Layer Flows: Their Structure and Measurement*. Oxford University Press.

KATUL, G. G., LI, D., CHAMECKI, M. & BOU-ZEID, E. 2013 Mean scalar concentration profile in a sheared and thermally stratified atmospheric surface layer. *Phys. Rev.* E **87** (2), 023004.

KATUL, G. G., PORPORATO, A., SHAH, S. & BOU-ZEID, E. 2014 Two phenomenological constants explain similarity laws in stably stratified turbulence. *Phys. Rev.* E **89** (2), 023007.

KOLMOGOROV, A. N. 1941 The local structure of turbulence in an incompressible fluid at very high Reynolds numbers. *Dokl. Akad. Nauk SSSR* **30**, 301–305.

LI, D. & BOU-ZEID, E. 2011 Coherent structures and the dissimilarity of turbulent transport of momentum and scalars in the unstable atmospheric surface layer. *Boundary-Layer Meteorol.* **140** (2), 243–262.

LI, D., KATUL, G. G. & BOU-ZEID, E. 2012 Mean velocity and temperature profiles in a sheared diabatic turbulent boundary layer. *Phys. Fluids* **24** (10), 105105.

LI, D., KATUL, G. G. & BOU-ZEID, E. 2015*a* Turbulent energy spectra and cospectra of momentum and heat fluxes in the stable atmospheric surface layer. *Boundary-Layer Meteorol.* **157** (1), 1–21.

LI, D., KATUL, G. G. & ZILITINKEVICH, S. S. 2015*b* Revisiting the turbulent Prandtl number in an idealized atmospheric surface layer. *J. Atmos. Sci.* **72** (6), 2394–2410.

LI, D., SALESKY, S. T. & BANERJEE, T. 2016 Connections between the Ozmidov scale and mean velocity profile in stably stratified atmospheric surface layers. *J. Fluid Mech.* **797**, R3.

LILLY, D. K. 1967 The representation of small scale turbulence in numerical simulation experiments. In *IBM Scientific Computing Symposium on Environmental Sciences*, pp. 195–210. White Plains.

LUMLEY, J. L. 1964 The spectrum of nearly inertial turbulence in a stably stratified fluid. *J. Atmos. Sci.* **21** (1), 99–102.

MASON, P. J. 1989 Large-eddy simulation of the convective atmospheric boundary layer. *J. Atmos. Sci.* **46** (11), 1492–1516.

MASON, P. J. & BROWN, A. R. 1999 On subgrid models and filter operations in large eddy simulations. *J. Atmos. Sci.* **56** (13), 2101–2114.

MOENG, C. H. & WYNGAARD, J. C. 1988 Spectral analysis of large-eddy simulations of the convective boundary layer. *J. Atmos. Sci.* **45** (23), 3573–3587.

MONIN, A. S. & OBUKHOV, A. M. 1954 Basic laws of turbulent mixing in the ground layer of the atmosphere. *Akad. Nauk. SSSR. Geofiz. Inst. Trudy* **151**, 163–187.

OBUKHOV, A. M. 1949 Structure of the temperature field in a turbulent flow. *Izv. Akad. Nauk SSSR Ser. Geogr. Geophys* **13**, 58–69.

PANCHEV, S. 1971 *Random Functions and Turbulence*. Pergamon.

PITSCH, H. & STEINER, H. 2000 Large-eddy simulation of a turbulent piloted methane/air diffusion flame (Sandia flame D). *Phys. Fluids* **12** (10), 2541–2554.

POPE, S. B. 2000 *Turbulent Flows*. Cambridge University Press.

PORTÉ-AGEL, F. 2004 A scale-dependent dynamic model for scalar transport in large-eddy simulations of the atmospheric boundary layer. *Boundary-Layer Meteorol.* **112** (1), 81–105.

PORTÉ-AGEL, F., PARLANGE, M. B., MENEVEAU, C. & EICHINGER, W. E. 2001 *A priori* field study of the subgrid-scale heat fluxes and dissipation in the atmospheric surface layer. *J. Atmos. Sci.* **58** (18), 2673–2698.

SADDOUGHI, S. & VEERAVALLI, S. 1994 Local isotropy in turbulent boundary layers at high Reynolds number flow. *J. Fluid Mech.* **268**, 333–372.

SCHUMANN, U. 1991 Subgrid length-scales for large-eddy simulation of stratified turbulence. *Theor. Comput. Fluid Dyn.* **2** (5–6), 279–290.

SCHUMANN, U., GRÖTZBACH, G. & KLEISER, L. 1980 Direct numerical simulation of turbulence. In *Prediction Methods for Turbulent Flows* (ed. W. Kollmann), vol. 1, pp. 123–258. Hemisphere.

SMAGORINSKY, J. 1963 General circulation experiments with the primitive equations: I. The basic experiment. *Mon. Weath. Rev.* **91** (3), 99–164.

SREENIVASAN, K. R. 1995 On the universality of the Kolmogorov constant. *Phys. Fluids* **7** (11), 2778–2784.

SREENIVASAN, K. R. 1996 The passive scalar spectrum and the Obukhov–Corrsin constant. *Phys. Fluids* **8** (1), 189–196.

STOLL, R. & PORTÉ-AGEL, F. 2006 Dynamic subgrid-scale models for momentum and scalar fluxes in large-eddy simulations of neutrally stratified atmospheric boundary layers over heterogeneous terrain. *Water Resour. Res.* **42** (1), W01409.

STOLL, R. & PORTÉ-AGEL, F. 2008 Large-eddy simulation of the stable atmospheric boundary layer using dynamic models with different averaging schemes. *Boundary-Layer Meteorol.* **126** (1), 1–28.

STULL, R. B. 1988 *An Introduction to Boundary Layer Meteorology*. Kluwer Academic.

TAYLOR, G. I. 1938 The spectrum of turbulence. *Proc. R. Soc. Lond.* A **132**, 476–490.

TENNEKES, H. & LUMLEY, J. L. 1972 *A First Course in Turbulence*. MIT Press.

VERCAUTEREN, N., BOU-ZEID, E., PARLANGE, M. B., LEMMIN, U., HUWALD, H., SELKER, J. & MENEVEAU, C. 2008 Subgrid-scale dynamics for water vapor, heat, and momentum over a lake. *Boundary-Layer Meteorol.* **128** (2), 205–228.